Search of the "second knee" by means of muon bundles in inclined EAS

I.I. YASHIN[1], A.G. BOGDANOV[1], D.V. CHERNOV[1], D.M. GROMUSHKIN[1], R.P. KOKOULIN[1], G. MANNOCCHI[2], A.A. PETRUKHIN[1], O. SAAVEDRA[3], V.V. SHUTENKO[1], G. TRINCHERO[2]
[1]*National Research Nuclear University MEPhI, 115409, Moscow, Russia*
[2]*Istituto di Fisica dello Spazio Interplanetario, INAF, 10133, Torino, Italy*
[3]*Dipartimento di Fisica Generale dell'Universita di Torino, 10125, Torino, Italy*
IIYashin@mephi.ru
DOI: 10.7529/ICRC2011/V01/0317

Abstract: Results of the study of primary cosmic ray flux characteristics in the energy range $10^{16} - 10^{18}$ eV by means of muon component of inclined EAS are presented. The method is based on the analysis of local muon density spectra (LMDS) obtained at ground level in a wide range of zenith angles from experimental data on muon bundles detected with coordinate-tracking detector DECOR. A special attention is paid to the energy region around 10^{17} eV where the existence of the second "knee" is predicted by various theoretical models. Comparison of experimental local muon density spectra and spectra calculated assuming different models of primary CR flux and hadronic interactions is given. Three different approaches to the data analysis revealed the change of the slope of LMDS in the primary energy range around 10^{17} eV.

Keywords: Cosmic rays, muons, muon bundles, extensive air showers, coordinate detector, streamer tube chambers, Cherenkov water detector.

1 Introduction

The main objective of the Russian-Italian experiment NEVOD-DECOR is the study of characteristics of the flux and interaction of primary cosmic rays (PCR) by means of a new EAS observable – local muon density spectra (LMDS) on the Earth's surface [1 - 3]. The approach based on ground-level measurements of muon bundles at various zenith angles and multiplicities for investigations of UHE cosmic rays in a very wide primary energy range (10^{15} - 10^{19} eV) was proposed and developed in [4, 5]. For the realization of the new method, the experimental complex including large Cherenkov water detector NEVOD with inner volume 2000 m^3 [6] and deployed around it coordinate-tracking detector DECOR with large area and precise spatial and angular resolution [7] is used. In the paper, results of investigation of PCR flux in the energy range $10^{16} - 10^{18}$ eV on the basis of the measured LMDS are presented. In this energy range the existence of the second knee is predicted by various theoretical models.

Due to the properties of the atmosphere, at large zenith angles the transverse area of showers (mainly muons at ground level) generated by UHE primary particles exceeds square kilometers, which is sufficient to explore primary energies of 10^{18} eV and even higher. Hence, muon detector may be considered as a point-like probe and capability of UHE primary particles detection is determined not by the size of the setup but by effective EAS dimensions in a plane orthogonal to the shower axis. The observed muon bundle multiplicity m is related to the local muon density D (measured in particles/m^2) as $D \sim m/S_{det}$. The integral spectrum of the events in local muon density (without taking into account fluctuations of the shower development), may be written as:

$$F(\geq D) = \int N(\geq E(\mathbf{r}, D))\, dS, \qquad (1)$$

where $\mathbf{r}$ is the point in the transverse section of the shower, $N(\geq E)$ is the integral primary energy spectrum, and the minimal primary energy E is defined by the equation $\rho(E, \mathbf{r}) = D$, where $\rho(E, \mathbf{r})$ is muon lateral distribution function (LDF) in a plane orthogonal to the shower axis. The analysis of local muon density spectra [5] has shown that these spectra exhibit a power type behavior with index β somewhat steeper than that of primary particles ($\beta = \gamma/\kappa \sim 2$; $\kappa \sim 0.9$). Contribution to the flux of events with a fixed local density is given by the showers with different energies detected at different (random) distances from the axis; however, due to a rapid decrease of cosmic ray flux, the interval of effective primary energies appears relatively narrow (Fig. 1). As seen from the picture, fixed densities at different zenith angles correspond to substantially different energies of primary particles; therefore measurements of LMDS in a wide range of zenith angles provide the possibility to simultaneously study cosmic ray characteristics in a very wide range of energies (up to 10^{18} eV and higher) in a single experiment.

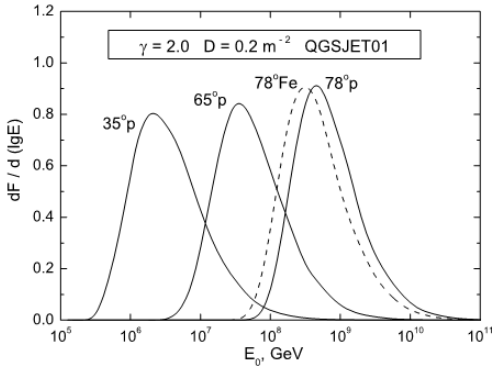

Figure 1. Contribution of various primary energies to events with fixed muon density at different zenith angles. Marks (p, Fe) indicate primary nuclei. Primary spectrum with the integral slope $\gamma = 2$ is assumed.

2 Experimental data

The coordinate detector DECOR [7] represents a multilayer system of plastic streamer tube chambers deployed around Cherenkov water calorimeter NEVOD [6]. The side part of DECOR includes eight eight-layer assemblies (supermodules, SM) of total area 70 m^2 with the angular accuracy of track reconstruction better than 0.7° and 0.8° for projected zenith and azimuth angles, respectively. The selection of muon bundles involves several stages [5]: trigger selection (coincidence of signals from any three SM); program selection of events with quasi-parallel tracks; final event classification and track counting by the operators. Muon energy threshold is close to 2 GeV. Experimental data accumulated during 2002-2007 (19922 h observation time) have been used for the present analysis.

A procedure of the analysis of data on muon bundles [5] includes: iterative deconvolution of muon bundle distributions to detector-independent muon density spectra for certain zenith angles; calculations of muon LDF for different hadronic interaction models with CORSIKA [8]; convolution of LDF with some model of primary spectrum and composition; comparison of measured and calculated LMDS. As a model of all-particle primary flux, a power type spectrum $dN/dE = 5.0\ (E,\ \mathrm{GeV})^{-2.7}$ $\mathrm{cm^{-2}s^{-1}sr^{-1}GeV^{-1}}$ below the knee energy (4 PeV) steepening to $(\gamma + 1) = 3.1$ above the knee was used. Significant influence on characteristics of muon bundle distributions at ground level has the geomagnetic field. It distorts the LDF of EAS muons and leads to a decrease of bundle intensity, the effect value being rapidly increased with zenith angle; therefore all calculations nave been performed taking into account the Earth's magnetic field.

3 Study of the primary cosmic ray energy spectrum behavior

Connection between the spectrum of events in local muon density and CR energy spectrum follows from equation (1). For a power type integral primary energy spectrum $N(\geq E) = A \cdot (E/E_0)^{-\gamma}$ and a scaling lateral distribution function of muons around some primary energy E_0, $\rho(E,\mathbf{r}) = (E/E_0)^{\kappa}\, \rho(E_0,\mathbf{r})$, the integral spectrum of events in muon density may be written as

$$F(\geq D) = N_0 (D/D_0)^{-\beta} \int [\rho(E_0,\mathbf{r})/D_0]^{\beta} dS,\ \beta = \gamma/\kappa. \quad (2)$$

In this case, for a certain zenith angle the following equation may be written:

$$N(\geq E_0) = N_0 = F(\geq D_0) \Big/ \int [\rho(E_0,\mathbf{r})/D_0]^{\beta} dS, \quad (3)$$

where N_0 is integral intensity of primary CR ($\mathrm{m^{-2}s^{-1}sr^{-1}}$). Thus, for the reconstruction of the intensity of primary flux it is necessary to know muon LDF, which is determined by the type of a parent particle and hadronic interaction model. The index of LMDS slope can be obtained directly from experimental distributions.

There are three possibilities to study features of PCR energy spectrum by means of LMDS: the analysis of the dependence of the slope of LMDS on primary particles energy; comparison of measured and calculated LMDS (for a set of certain models of primary spectrum, composition and hadronic interactions); reconstruction of PCR energy spectrum by means of (3) (again, under certain assumptions about composition and model of hadronic interaction) from experimental LMDS.

3.1 Analysis of LMDS shape

Differential LMDS (multiplied by D^3) for three zenith angles (35°, 50° and 65°) are shown in Fig. 2. The curves correspond to two extreme versions of primary composition (only protons and only iron nuclei) and two combinations of hadronic interaction models available in CORSIKA: QGSJET01+ GHEISHA and SIBYLL2.1+ FLUKA. As a del of all-particle primary flux, a power type spectrum with the knee at 4 PeV as described above was used. Arrows in the upper part of the figures indicate estimated log-average primary energies responsible for generation of muon bundles with given densities; these estimates only slightly depend on primary particle type and interaction model. At moderate zenith angles (35°, Fig. 2a), the steepening of the spectra related with the knee is seen both in data and calculations; a reasonable agreement (including the absolute normalisation) of DECOR data with CORSIKA-based simulation is observed. Data for 65° (Fig. 2c) correspond to intermediate primary energies (about 3 – 500 PeV). In this angular interval, the behavior of experimental LMDS demonstrates a trend to a heavier composition and a hint for an increase of the slope near 10^{17} eV: partial fits of the data above and below this energy (thin lines in the figure) give $\Delta\beta = 0.20 \pm 0.10$. Fit of the "tail" of the experimental spectrum for 50° (Fig. 2b) has practically the same slope as the part of the spectrum for 65° below the second knee. It allows to exclude the version of methodical origin (track shadowing) of the second knee in the local density spectrum.

3.2 Combined estimator of primary energy

The preceding analysis was based on LMDS obtained in relatively wide bands of zenith angles. However, the effective energy of primary particles strongly depends on zenith angle. To enhance the sensitivity to the shape of primary CR spectrum (first of all, to verify the existence

of the "second knee"), an event-by-event analysis on the basis of a combined estimator of primary particle energy E_{EST} was performed.

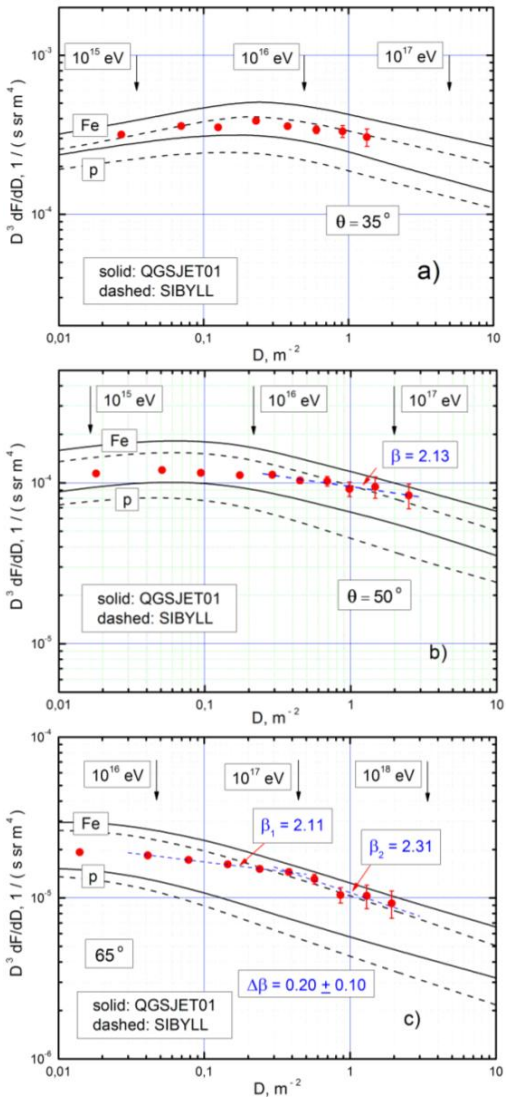

Figure 2. LMDS for different zenith angles. Points - DECOR data; curves - calculations. a) θ = 35°; b) θ = 50°; dotted line represents partial fit of the data between 10^{16} and 10^{17} eV; c) θ = 65°; dotted lines represent partial fits of the data below and above 10^{17} eV.

The results of calculations of the average logarithms of the energy of primary protons (in frame of the above assumptions about energy spectrum and QGSJET01 model) are presented in Figs. 3 and 4 as functions of lg$D$ and lg(cosθ). In certain ranges of densities (0.05 - 2.0 m^{-2}), zenith angles (40 - 80°) and primary energies (10^{16} - 10^{18} eV) the dependences in Fig.s 3 and 4 are well approximated by power law functions:

$$(E_{EST}/E_0)=(D/D_0)^{1.07}\cdot(\sec\theta/\sec\theta_0)^{3.8}. \qquad (4)$$

Taking as a reference point the energy $E_0 = 10^8$ GeV and zenith angle θ_0 = 65°, we can find (by interpolation of calculated curves) D_0 = 0.377.

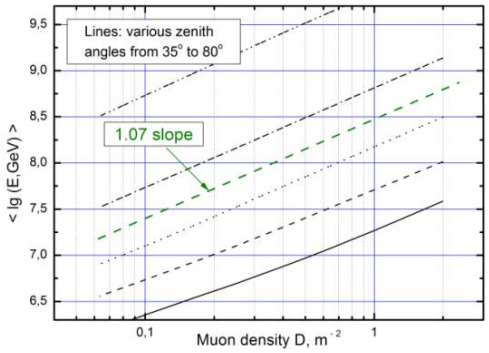

Figure 3. Dependence of average logarithm of primary energy on lg(D) for different zenith angles.

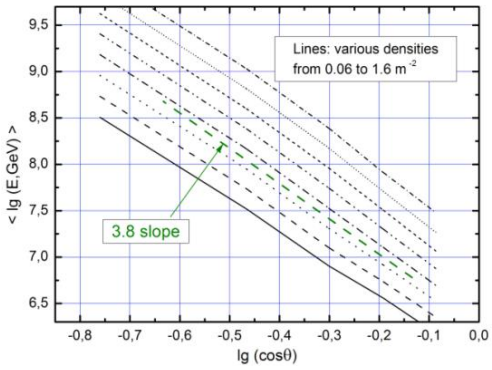

Figure 4. Dependence of average logarithm of primary energy on lg(cosθ) for different muon densities.

In this case, the expression (4) for primary energy estimation may be re-written as follows:

$$\lg(E_{EST},\ \text{GeV}) = 8.00 + 1.07\ (\lg D + 0.424) - 3.80\ (\lg\cos\theta + 0.374). \qquad (5)$$

This function reproduces calculation data in the above ranges of densities and zenith angles with accuracy about 2% (in energy), and it is used for the event-by-event analysis as a primary energy estimator $E_{EST}(m, \theta, \varphi)$.

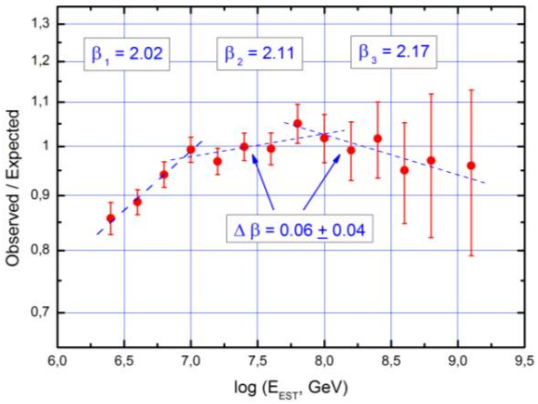

Figure 5. Ratio of experimental and expected distributions of primary energy estimations (events with $5 \le m \le 55$ and $40^o \le \theta \le 80^o$).

In Fig. 5 the ratio of experimental and calculated distributions of estimates of energy responsible for generation of muon bundles with multiplicities $5 \le m \le 55$ and zenith angles $40^o \le \theta \le 80^o$ is presented. Expected distributions were calculated for constant index of LMDS

β = 2.13 (without the knee). A smooth slope variation below $E_{EST} = 10^7$ GeV (close to the first knee) and a hint for the increase of the slope at $E_{EST} > 10^8$ GeV are clearly seen. This ratio was fitted by power law functions for different intervals of E_{EST}. Fitting results presented in Fig. 5 evidence for a gradual increase of power law index in the given range of E_{EST}. However, the difference of indices obtained around 10^8 GeV ($\Delta\beta = 0.06 \pm 0.04$) is appreciably less than the value obtained as a result of partial fits of differential local muon density spectra for zenith angle 65º (Fig. 2b, $\Delta\beta = 0.20 \pm 0.10$).

3.3 Dependence of LMDS slope index on the primary energy

The dependence of the experimentally obtained values of the LMDS slope index on the effective energy of primary CR particles is given in the Fig. 6. Different symbols correspond to sub-sets of events for different intervals of zenith angles. As it is seen from the figure, estimations of the LMDS slopes β obtained at different angles well agree with each other in the overlapping ranges of energies. Indicated errors in ordinate are statistical. Horizontal error bars correspond to the rms-spread of primary energies which give contribution to the different data points (typically, $\sigma_{\lg E} \approx 0.4$).

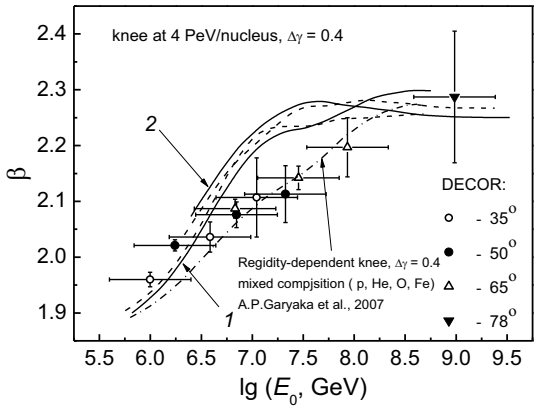

Figure 6. Dependence of LMDS slope index on the average logarithm of primary energy. Solid and dashed curves – calculations for protons and iron nuclei (1 and 2 – for zenith angles 50° and 65° correspondingly) with the knee at E_{knee}=4 PeV/nucleus. Dash-dotted curve – mixed composition (4 species of nuclei) with the knee at a fixed rigidity (E_{knee}/Z =2.5 PeV).

In the analyzed interval of primary energies (10^{15} - 10^{18} eV) the value of β gradually increases from ~ 1.9 to ~ 2.3. Taking into account the approximate relation of slope indices of primary CR spectra and LMDS, it corresponds to a change of the index of primary spectrum from ~ 1.7 to ~ 2.1. Solid and dashed curves in the figure represent the behavior of the expected spectrum index under assumption of one-component primary composition (protons or iron) with the knee at the same energy E_{knee} = 4 PeV. It is seen that such a supposition contradicts the data. A gradual increase of LMDS slope in the range 10^{15} – 10^{18} eV could be better described assuming the presence of several primary mass species with mass-dependent or rigidity-dependent knee position [9] (dash-dotted curve).

4 Conclusion

Analysis of local muon density spectra for different zenith angles has revealed some important features of their shape: steepening of LMDS related with the knee of primary CR spectrum at PeV energies; a trend to a heavier composition at higher energies; a hint for an increase of the slope near 10^8 GeV. To obtain additional information about these features, a new technique based on a combined estimator matching a certain muon density and zenith angle with an effective energy of primary particle was applied. This method also reveals the steepening of the spectrum around 10^8 GeV but with a smaller slope change. The obtained dependence of LMDS slope index on primary energy in the range 10^{15} – 10^{18} eV exhibits gradual increase from ~ 1.9 up to ~ 2.3 that corresponds to the change of γ of CR integral spectrum from ~ 1.7 to ~ 2.1. Unfortunately, significant error of primary energy determination ($\sigma_{\lg E} \approx 0.4$) does not allow study features of the spectrum more precisely. Nevertheless, comparative analysis of experimental and expected LMDS gives a possibility to study characteristics of the PCR flux in a wide energy range (more than three decades in primary particle energy) on the basis of a single technique and by means of a single experimental setup.

5 Acknowledgments

The research is performed in the Scientific and Educational Centre NEVOD (MEPhI) and has been supported by Russian Ministry of Education and Science (leading scientific school grant NSh-5712.2010.2).

6 References

[1] I.I. Yashin, M.B. Amelchakov, N.S. Barbashina et al. Int. J. Mod. Phys., 2005, v. A 20, pp. 6937-6941.
[2] N.S.Barbashina et al. Nucl. Phys. B (Proc. Suppl.), 2007, v. 165, pp. 317-321.
[3] A.G.Bogdanov et al. Nucl. Instr. Meth. in Phys. Res. A, 2008, v. 588, no. 1-2, pp. 189 - 193.
[4] M.B.Amelchakov et al. Physics of Atomic Nuclei, 2007, v. 70, no. 1, pp. 175-183.
[5] A.G.Bogdanov et al. Physics of Atomic Nuclei, 2010, v. 73, no. 11, pp. 1904 - 1920.
[6] V.M. Aynutdinov et al., Astrophysics and Space Science, 1998, v. 258, pp. 105-115.
[7]. M.B. Amelchakov et al., Proc. 27th ICRC, 2001, v. 3, pp. 1267-1271.
[8] D. Heck et al., Forschungszentrum Karlsruhe, Report FZKA, 6019, 1998, Karlsruhe.
[9] A.P. Garyaka et al. Astropart. Phys., 2007, v. 28, pp. 169 -181.